

On the detonation of a methane-oxygen mixture in a plane-radial chamber

D.V.VORONIN

Lavrentyev Institute of Hydrodynamics of SB RAS,
Lavrentyev str, 15, 630090 Novosibirsk
RUSSIA

Abstract. - Numerical modeling of the formation, subsequent ignition, and development of the detonation process in methane-oxygen mixtures within a flat radial chamber is performed using the Reynolds equations. Fuel and oxidizer are supplied separately to the chamber through valves in its rigid walls. The main equations are based on two-dimensional, non-stationary conservation laws for mass, momentum, and energy of a compressible, chemically reacting gas. The model accounts for turbulence and diffusion processes in multicomponent mixtures. It is shown that a self-sustaining detonation process occurs in the chamber even at relatively small shock wave amplitudes. The detonation wave parameters are largely determined by the mixing rate of the reacting components and the ability to reach ignition concentration limits.

Key words: - modeling, methane, chemical reaction, continuous detonation, mixing

Received: April 23, 2024. Revised: April 8, 2025. Accepted: June 2, 2025. Published: August 5, 2025.

1 Introduction

Most modern rocket engines operate under constant pressure conditions. This is the so-called isobaric cycle, or deflagration, which results in slow burning of fuel. This type of burning does not require a robust chamber design, but increasing the engine's efficiency is necessary.

Detonation processes are usually considered an undesirable mode of operation. However, using detonation mode for fuel burning instead of an isobaric cycle is desirable for enhancing the engine's main characteristics. On the one hand, detonation results in the appearance of shock waves with a reaction zone behind them, which requires more robust conditions for the entire system. On the other hand, detonation combustion is 25% more efficient than deflagration, resulting in less fuel consumption. The velocity of reactive gases can be increased by 20-25 times.

Paper [1] was devoted to the theoretical basis of the possibility of such an engine. A review of modern theoretical and practical investigations can be found in [2]. Paper [3], for example, is also devoted to the creation of such an engine. One of the most important aspects of the problem is the geometrical form of the chamber. A comparison of different geometrical types of combustion chambers was done in paper [4] from the point of view of their efficiency. Determination of the optimal operating modes of the chamber requires the creation of detailed mathematical models.

When modeling flows in the combustion chamber, it is very important to take into account the processes of viscosity, thermal conductivity, and turbulent mixing of components. For mixtures of methane with oxygen, such a problem has not yet been solved for such a chamber. This paper is devoted to the mathematical study of the initial stage of detonation excitation in a plane radial chamber for methane–oxygen gaseous mixtures.

2 Problem Formulation

The scheme of the device can be seen in Fig. 1. The chamber represents a plane ring body generated by the rotation of a rectangular segment around the symmetry axis Z , which passes through the origin (0-point in Fig. 1). The outer (maximal) diameter of the body is 200 mm, and the inner (minimal) diameter is 100 mm. We have empty space around the origin. Inside the device, there is a zone of chemical transformations with a rectangular cross-section between metallic plane surfaces P_3 . The distance between the surfaces is 10 mm. Surface P_2 is a rigid metallic wall where three round inlet slots are disposed. Two outer slots are inlet nozzles for fuel (methane), and the middle slot is an inlet nozzle for oxidizer (oxygen). The exit of detonation products into open space takes place through surface P_1 (the outlet zone of the chamber). The Z -axis is the axis of symmetry of the body, and the R -axis is at a right angle to the Z -axis. Combustion of the mixture takes place inside the chamber. Initially, the internal volume of the

installation is filled with nitrogen at an initial gas pressure of $p_0 = 1$ atm and a temperature of $T_0 = 300$ K. The initial velocity of the medium is zero. Oxygen in the channel is supplied from the receiver through the middle slot in surface P_2 . Methane enters the chamber through the other two slots on P_2 . The fuel and oxidizer enter the chamber separately and mix inside. The gas in the receivers is at elevated pressure values of 5 atm, temperature T_0 , and zero velocity. The methane jets are directed to meet the oxygen jet at an angle of 45 degrees to surface P_2 . The direction of the oxygen jet is at a right angle to surface P_2 . Such a disposition of slots is required for better mixing of reacting materials. The angle also ensures rotational motion of the gas mixture in the chamber. The form and parameters of the chamber correspond to the experimental facility [2]. At the initial instant $t_0 = 0$, the valves are removed, and the reacting gas comes from the receivers into the chamber. Some time is required to supply the necessary mixing of reacting materials; after the delay, a concentrated release of outer energy takes place in the mixing zone that ignites the mixture and results in the start of detonation processes within the chamber. It is necessary to find the values of the gas parameters in the chamber after ignition at $t > 0$.

Unsteady motion of viscous compressible turbulent fluid was described by Reynolds equations [5] for the laws of conservation of mass, momentum, and energy, taking into account the effects of turbulence:

$$\frac{\partial \mathbf{A}}{\partial t} + \frac{\partial \mathbf{B}}{\partial r} + \frac{\partial \mathbf{C}}{\partial z} = \mathbf{D}, \quad (1)$$

where r, z – radial and axial (along symmetry axis) cylindrical coordinates. For the vector functions $\mathbf{A}, \mathbf{B}, \mathbf{C}, \mathbf{D}$ we have

$$\mathbf{A} = \begin{pmatrix} r\rho \\ r\rho u_r \\ r\rho u_\theta \\ r\rho u_z \\ rE \end{pmatrix}, \mathbf{B} = \begin{pmatrix} r\rho u_r \\ r(\rho u_r^2 + p - \tau_{11}) \\ r(\rho u_r u_\theta - \tau_{12}) \\ r(\rho u_r u_z - \tau_{13}) \\ r(E + p)u_r - r(u_r \tau_{11} + u_\theta \tau_{12} + u_z \tau_{13} + q_r) \end{pmatrix},$$

$$\mathbf{C} = \begin{pmatrix} r\rho u_z \\ r(\rho u_r u_z - \tau_{13}) \\ r(\rho u_\theta u_z - \tau_{23}) \\ r(\rho u_z^2 + p - \tau_{33}) \\ r(E + p)u_z - r(u_r \tau_{13} + u_\theta \tau_{23} + u_z \tau_{33} + q_z) \end{pmatrix},$$

$$\mathbf{D} = (0, \rho u_\theta^2 + p - \tau_{22}, -\rho u_r u_\theta + \tau_{12}, 0, 0),$$

the velocity vector has radial u_r , circumferential u_θ and axial u_z components; p, ρ, T and $\gamma = c_{p,1}/c_{v,1}$ are pressure, density, temperature and the ratio of specific heats, respectively; μ_e and λ_e are the effective viscosity and effective thermal conductivity of the gas. μ_e is a sum of molecular μ and turbulent μ_t viscosity, $\lambda_e = c_p(\mu/Pr + \mu_t/Pr_t)$, Pr and Pr_t are molecular and turbulent Prandtl numbers.

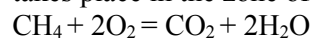
The components of the viscous stress vector τ_{ij} and the components of the heat flow vector q_r, q_z are defined similarly to [6]. Turbulence was described using a two-parameter $k - \epsilon$ model [7].

The change in the concentration of the i -th gas component due to space-time diffusion and chemical reactions was determined using Fick's second law:

$$\frac{\partial(r\rho C_i)}{\partial t} + \frac{\partial(r\rho u_r C_i)}{\partial r} + \frac{\partial(r\rho u_z C_i)}{\partial z} = r\rho D_i \left(\frac{\partial^2 C_i}{\partial r^2} + \frac{1}{r} \frac{\partial C_i}{\partial r} + \frac{\partial^2 C_i}{\partial z^2} \right) + r\rho H_i, \quad (3)$$

where D_i is the diffusion coefficient and H_i is the intensity of the substance sources due to chemical reactions.

A global reaction between methane and oxygen takes place in the zone of turbulent mixing:



A two-stage model of chemical kinetics was used. Start of chemical reactions occurs after the end of the chemical ignition delay t_{ign} . The beginning of ignition delay is a moment when we have the value of ignition temperature in the medium (here, $T_{ignition} = 1200\text{K}$). Chemical reactions take place only if concentrations of methane and oxygen lie between chemical reaction concentration limits (from 5 to 95 percent).

Boundary conditions:

For stiff walls of the chamber P_3 and stiff parts of P_2 , the conditions of gas adhesion and constant gas temperature are valid: $u_r = u_z = u_\theta = 0, T = T_0$.

At the inlet (the slots on surface P_2), the condition of adiabatic gas flow from the collectors is valid [7]:

$$V = \sqrt{\frac{2}{\gamma-1} c_0^2 \left(1 - \left(\frac{P_0}{P_r} \right)^{\frac{\gamma-1}{\gamma}} \right)}, \quad (4)$$

where V is the flow rate and C_0 is the velocity of sound in the collector gas; at the output (surface P_1) "soft boundary conditions" are satisfied (the first derivatives of the main functions are equal to zero).

3 Numerical solution of the problem

The system of equations (1) - (4) with the boundary conditions was solved numerically using the method of individual particles, an update of Harlow's particle-in-cell method [8]. A regular mesh was used, with the number of cells in a camera cross-section equal to 100. The number of particles in cells is variable. The numerical algorithm provides an opportunity for association and splitting of individual particles belonging to the same body, depending on the flow parameters. The maximal number of particles in a cell is equal to seven.

The calculations were performed for the following initial values of nitrogen: $p_0 = 1$ bar, $\rho_0 = 1.15$ kg/m³, $\gamma = 1.4$, $u_{r0} = u_{\theta 0} = u_{z0} = 0$; initial values of air pressure p_r and density ρ_r in the receiver: $p_r/p_0 = 5$, $\rho_r/\rho_0 = 5$.

In numerical simulations, we have three stages of the processes in the chamber. The initial (first) stage is the generation of a mixing zone of methane and oxygen without chemical reactions. The second stage is the input of outer energy to ignite the mixture and start chemical reactions. The third stage is the generation of a detonation wave in the zone.

Fig. 2 represents the numerical results of the first stage for pressure maps at different subsequent instants: $t_1 = 2.0 \cdot 10^{-5}$ s, $t_2 = 4.0 \cdot 10^{-5}$ s, $t_3 = 7.0 \cdot 10^{-5}$ s, $t_4 = 10.0 \cdot 10^{-5}$ s, $t_5 = 13.0 \cdot 10^{-5}$ s in a rectangular cross-section of the chamber. We can see 20 isobars here in a range from 1 atm to the maximal value. Three inlet slots are disposed on the bottom of the figure (P_2 surface). The middle one is a slot for oxygen, and the other two are for methane. The jets of fuel and oxidizer are coming from the bottom of the figure to the top, and they generate a shock wave in the direction of surface P_1 . At the t_1 instant, the maximal value of the pressure is 2.65 atm at the methane slots. At the t_2 instant, we have

$p_{\max} = 2.58$ atm; for the other instants, the value of p_{\max} is nearly the same. At the bottom corners of the chamber, the pressure values are low (about 0.9 atm) due to the high velocities of viscous methane jets.

The initial stage of velocity distribution can be seen in Fig. 3, where velocity u isolines are

presented. Here, $u = \sqrt{u_r^2 + u_\theta^2 + u_z^2}$. The

maximal value of velocity occurs at the slots on surface P_2 , and this value is close to one of sound velocity, approximately 330 m/s. At the rigid walls P_3 , the velocity is zero due to the no-slip condition for viscous flow. The mean velocity in the middle oxygen jet is greater than in the methane jets, since the gas in the oxygen jet is heavier and has a greater initial momentum. Furthermore, the no-slip condition influences the propagation of the methane jets. For these reasons, oxygen travels a greater distance from the slots than methane for the same time intervals.

Similar behavior can be seen in Fig. 4, where density isolines are presented for the same time intervals. The initial density of nitrogen in the camera is 1.15 kg/m³. The maximal value of density occurs inside the oxygen jet, approximately $\rho_{\max} = 3.5$ kg/m³. The minimal values of density occur inside the methane jets, approximately $\rho_{\min} = 1.7$ kg/m³. This is valid for all instants.

Isotherms for the same time intervals can be seen in Fig. 5. The temperature range here is [260K, 340K]. The greater values of temperature are at the tips of the jets, behind the leading shock wave. The smaller values are at the slots on surface P_2 . It is clear that the temperature level is not high enough here for the self-ignition of the reacting mixture in the camera. However, the most favorable temperature region for self-ignition exists, it is in the middle of the device.

Fig. 6 is devoted to the passage of two methane jets for different time intervals. One can see methane mass concentration isolines there, in the range [0, 1]. At the slots, the direction of the jets is 45 degrees with respect to the direction of the middle oxygen jet, to supply a better and sooner mixing zone. Because of the influence of the no-slip condition at the walls, the mean velocity of the gas inside the methane jets is less than that for oxygen. That results in the generation of methane/oxygen mixing zones not only at the sides of the jets but at their tips as well. Slowly disappearing zones of nitrogen are present at the right and left corners of the camera, close to the inlet surface P_2 . This means that no chemical reactions will occur in these areas.

Propagation of the middle oxygen jet can be seen in Fig. 7, where isolines of mass concentration of O_2 are presented in the range [0, 1]. It is clear that, by the moment the leading shock wave reaches the outlet surface P_1 , the jet has passed only 2/3 of the distance between the inlet and outlet surfaces of the chamber. Intense mixing of oxygen with nitrogen takes place at the top of the jet, and with hydrogen on both sides of the jet. By instant t_5 , the sizes of the fuel/oxidizer zone are large enough to support detonation processes after ignition.

The dynamics of nitrogen output from the chamber can be seen in Fig. 8 (due to the influence of methane and oxygen jets). N_2 mass concentration isolines are shown there in the range [0, 1]. However, by instant t_5 , nearly half of the chamber volume is still filled with inert gaseous nitrogen. As we will see later, this fact does not prevent the generation of a detonation wave inside the device.

At instant $t = 14 \cdot 10^{-5}$ s, external energy (a spark) was introduced into the mixing area at surface P_2 to ensure ignition of the combustible gas mixture. The gas temperature in the local energy input area should exceed the ignition temperature of about 1200 K, and the mass concentrations of fuel and oxidizer in the mixture in this area should lie within the range between the ignition concentration limits [5, 95] %. The subsequent combustion of methane with energy release ensures the initiation of the detonation process.

Fig. 9 shows the isolines of the mass concentration of substances in the chamber after ignition at the moment $t = 20 \cdot 10^{-5}$ s. It can be seen from the figure that, by this moment, almost all the pre-mixed methane has burned up to form shock waves, but new portions of fuel continue to flow through holes in surface P_2 , ensuring the continuity of the detonation process. Some of the unreacted oxygen in the jet has almost reached the outlet surface P_1 . A small part of the inert nitrogen still remains inside the chamber. At the same time, the chamber begins to fill with chemical reaction products CO_2 and H_2O on the sides of the oxygen jet. In the future, they will begin to leave the chamber through surface P_1 . The maximum value of the mass concentration of carbon dioxide at this moment is 0.32, and the maximum of the mass concentration of water vapor is 0.28.

Fig. 10 depicts the distribution of main thermodynamical parameters at the same instant. Chemical reactions occur only in the zone of fuel/oxidizer mixing. The maximum value of the rate of chemical reaction is $8.76 \text{ kg}\cdot\text{moll}/(\text{m}^3 \text{ s})$

here. The detonation wave is quite weak; the pressure value is not greater than 4 atm. In comparison, the pressure value in the wave for the Chapman-Jouguet regime is about 14 atm. The reason for the difference is that methane concentration varies for different points of the area, not all portions of methane are burning, and the heat release is mainly defined by the rate of mixing. Besides, the rarefaction wave is coming inside the camera from outer space through the surface P_1 . Values of temperature reach 2000 K in the reaction zone and ensure continuity of detonation. The gas velocity maximum is close to the sonic value and takes place in the middle of the device.

4 Conclusion

Numerical modeling of the formation, subsequent ignition, and development of the detonation process of methane-oxygen mixtures in a flat radial chamber is performed within the framework of the Reynolds equations. Fuel and oxidizer are supplied to the chamber separately through valves in the rigid walls of the chamber. The main equations are based on two-dimensional nonstationary laws of conservation of mass, momentum, and energy of a compressible chemically reacting gas. The model takes into account the processes of turbulence and diffusion of multicomponent mixtures. It is shown that a self-sustaining detonation process occurs in the chamber at relatively small values of the amplitude of shock waves. The parameters of the detonation wave are largely determined by the mixing rate of the reacting components and the possibility of reaching ignition concentration limits.

References

- [1] Wojciechowski, B. W. Stationary detonation, Dokl. *USSR Academy of sciences*. 1959. Vol. 129, No. 6. P. 1254 - 1256.
- [2] Bykovskii F. A., Zhdan S. A. *Continuous spin detonation*. Novosibirsk. Publishing house of SB RAS. 2013.
- [3] Frolov, S. M., Ivanov V. S and others. The afterburning of the detonation combustion chamber. *Reports of the Russian Academy of Sciences*, 2020, vol. 490, p. 82-86.
- [4] Voronin D.V. On the optimal choice of type of combustion chamber for the initiation of gas detonation - *WSEAS Transactions on Fluid Mechanics*. 2023. V.18. P.109-113. DOI: 10.37394/232013.2023.18.11.

[5] Anderson D., Tannehill J., Pletcher R. *Computational fluid mechanics and heat transfer*, New York, Hemisphere, 1984.

[6] Voronin D. V. On the self-ignition of gas in the flat vortex camera. *Physics of combustion and explosion*. 2017. Vol. 53, No. 5. P. 24-30.

[7] Loitsyanskii L. G. *Mechanics of Liquids and Gases*. Pergamon Press, Oxford, New York, 1966.

[8] Belotsercovskii O.M., Davydov Yu.M. *Method of large particles in gas dynamics*, Moscow, Nauka, 1984.

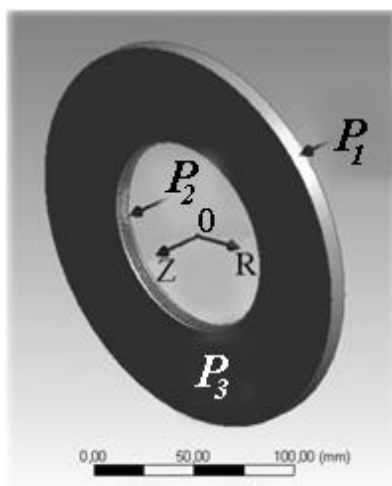


Fig. 1. The scheme of the vortex chamber.

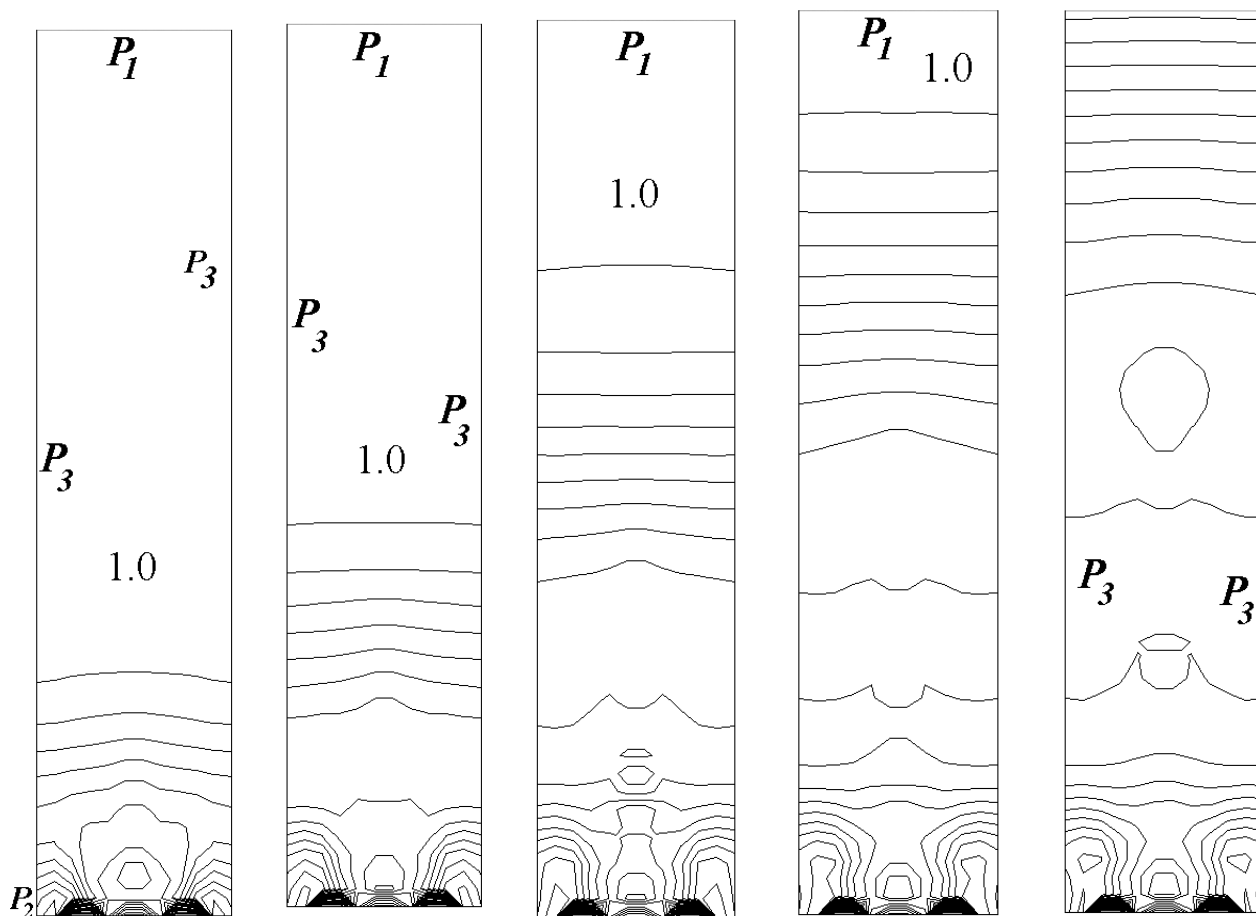


Fig.2. Evolution of pressure maps (atm) for instants: $t_1 = 2.0 \cdot 10^{-5}$ s, $t_2 = 4.0 \cdot 10^{-5}$ s, $t_3 = 7.0 \cdot 10^{-5}$ s, $t_4 = 10.0 \cdot 10^{-5}$ s, $t_5 = 13.0 \cdot 10^{-5}$ s.

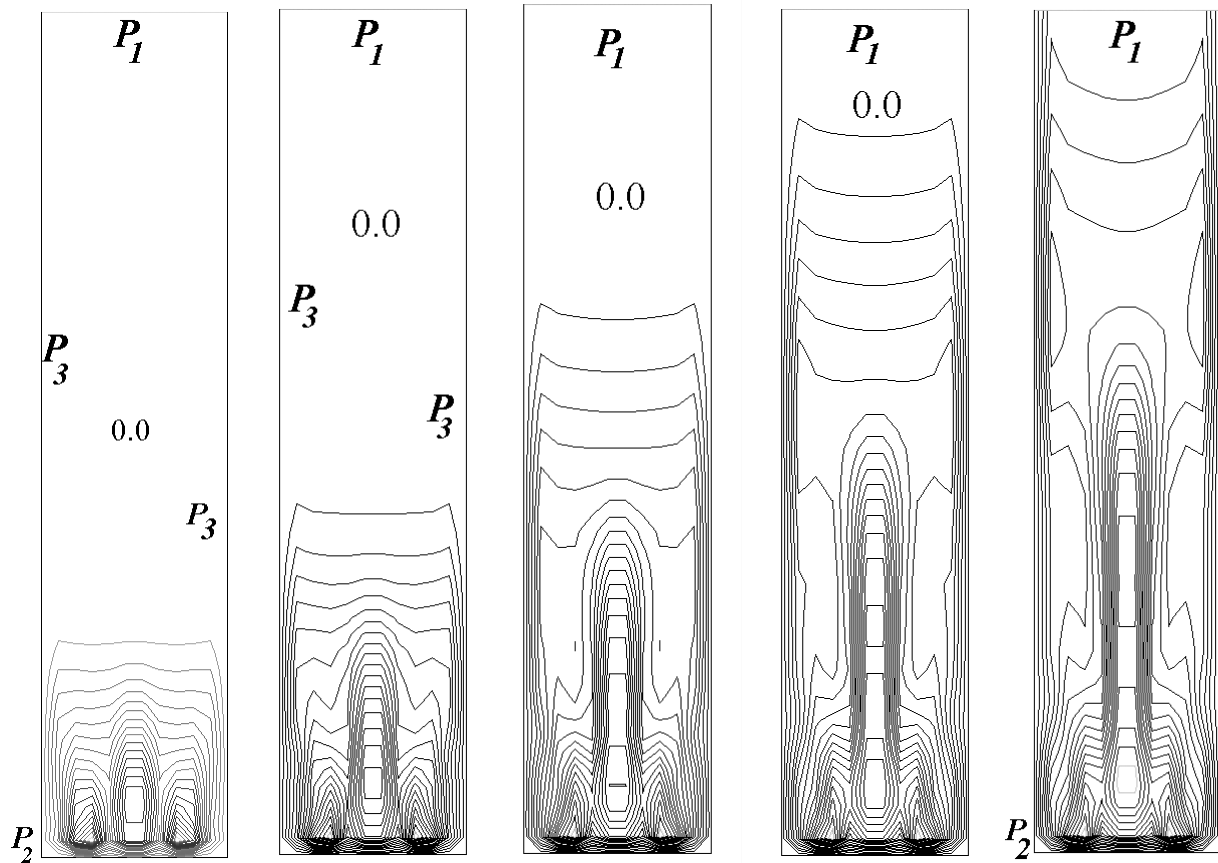


Fig. 3. Evolution of velocity maps (u , m/s) for instants: t_1, t_2, t_3, t_4, t_5 .

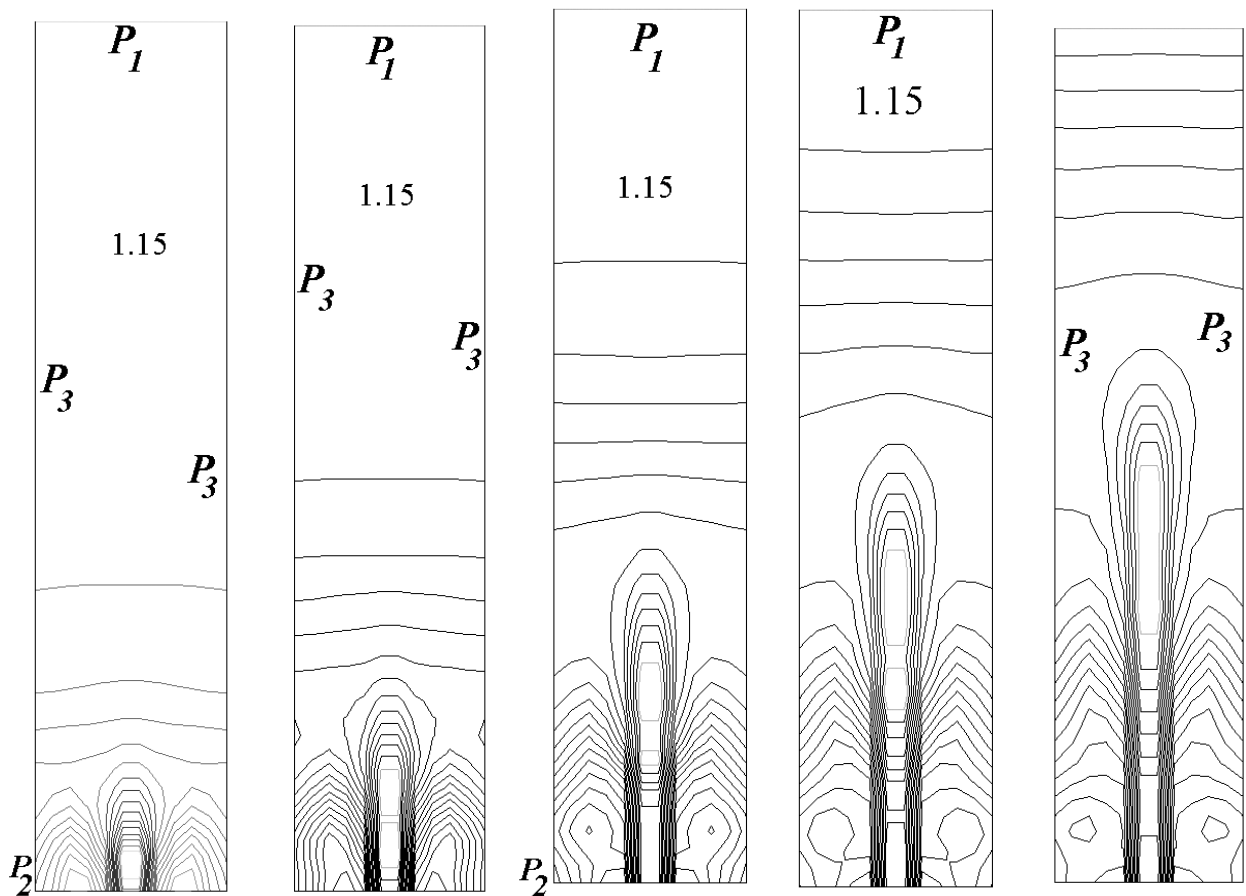


Fig. 4. Evolution of density maps (kg/m^3) for instants: t_1, t_2, t_3, t_4, t_5 .

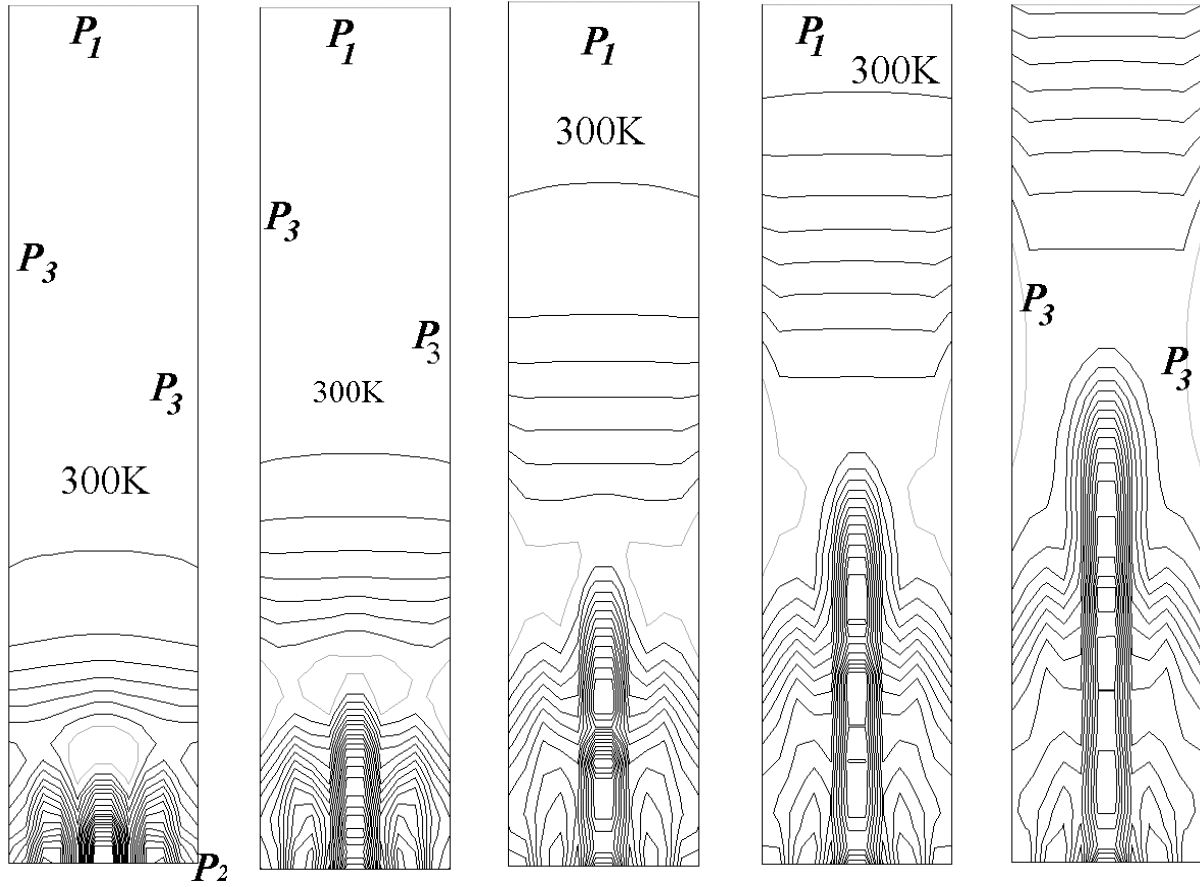


Fig. 5. Evolution of temperature (K) maps for instants: t_1, t_2, t_3, t_4, t_5 .

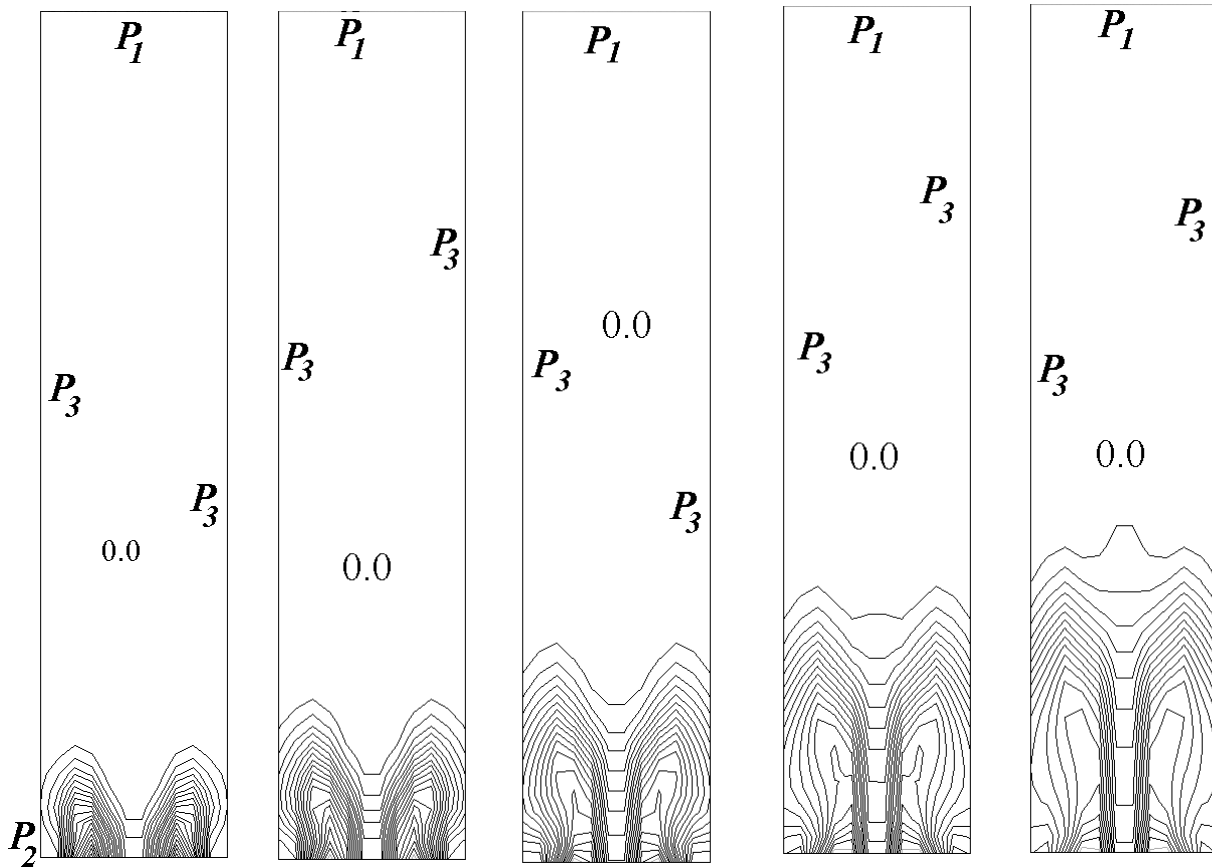


Fig. 6. Evolution of methane mass concentration maps for instants: t_1, t_2, t_3, t_4, t_5 .

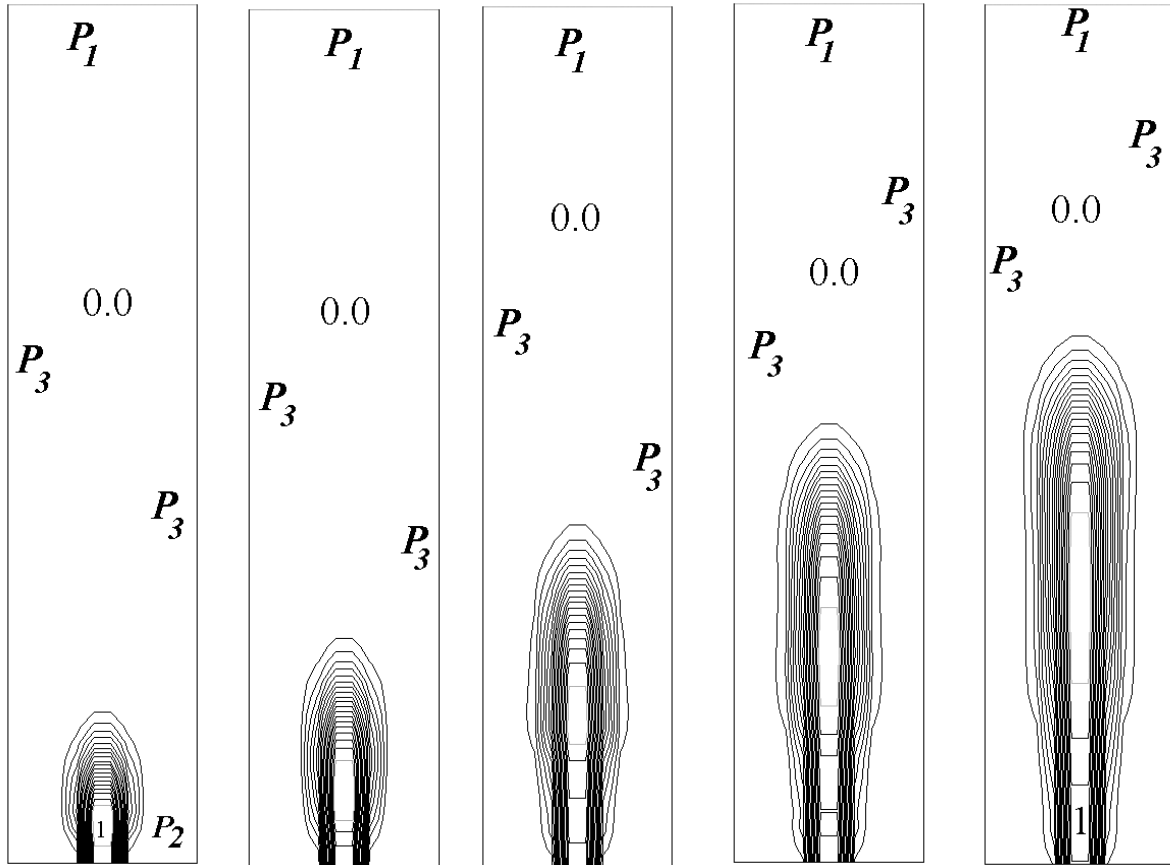


Fig. 7. Evolution of oxygen mass concentration maps for instants: t_1, t_2, t_3, t_4, t_5 .

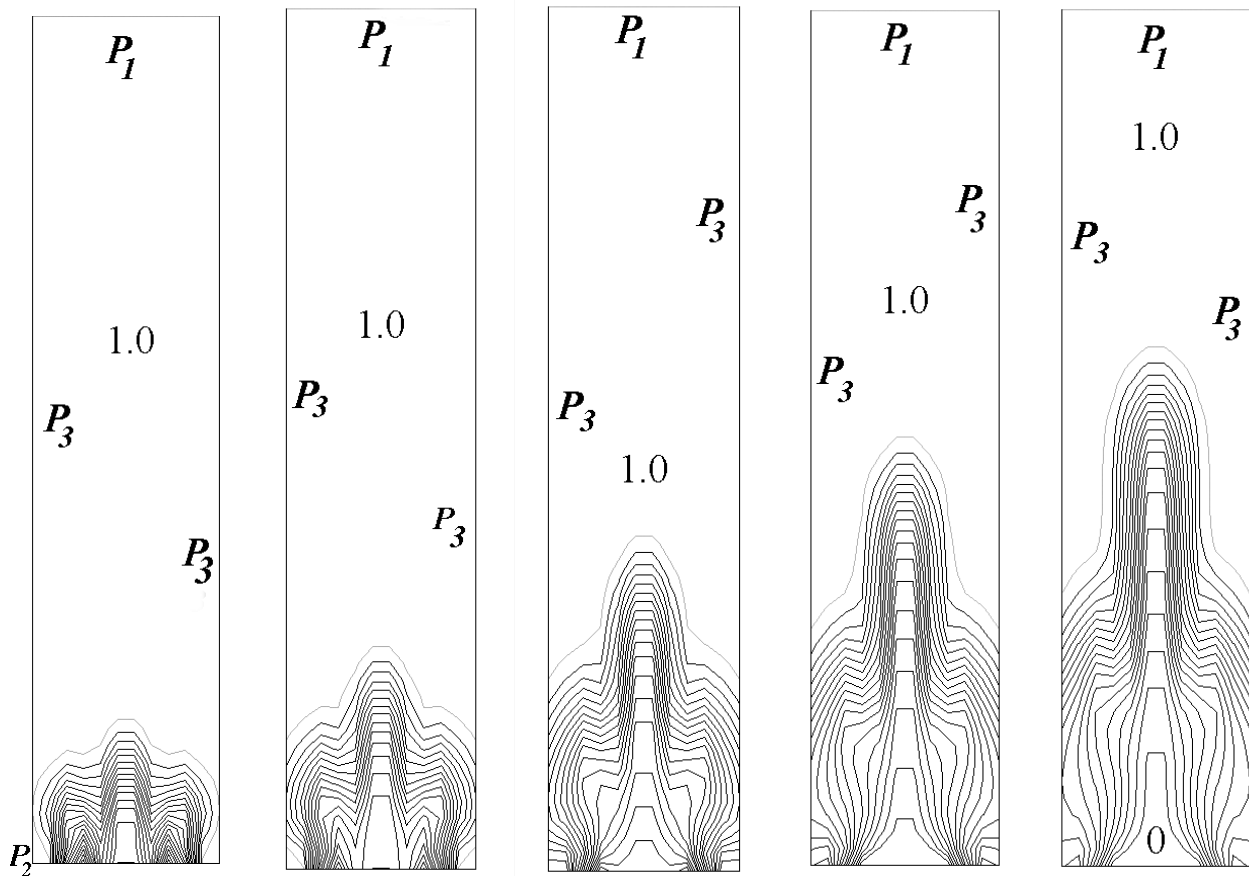


Fig. 8. Evolution of nitrogen mass concentration maps for instants: t_1, t_2, t_3, t_4, t_5 .

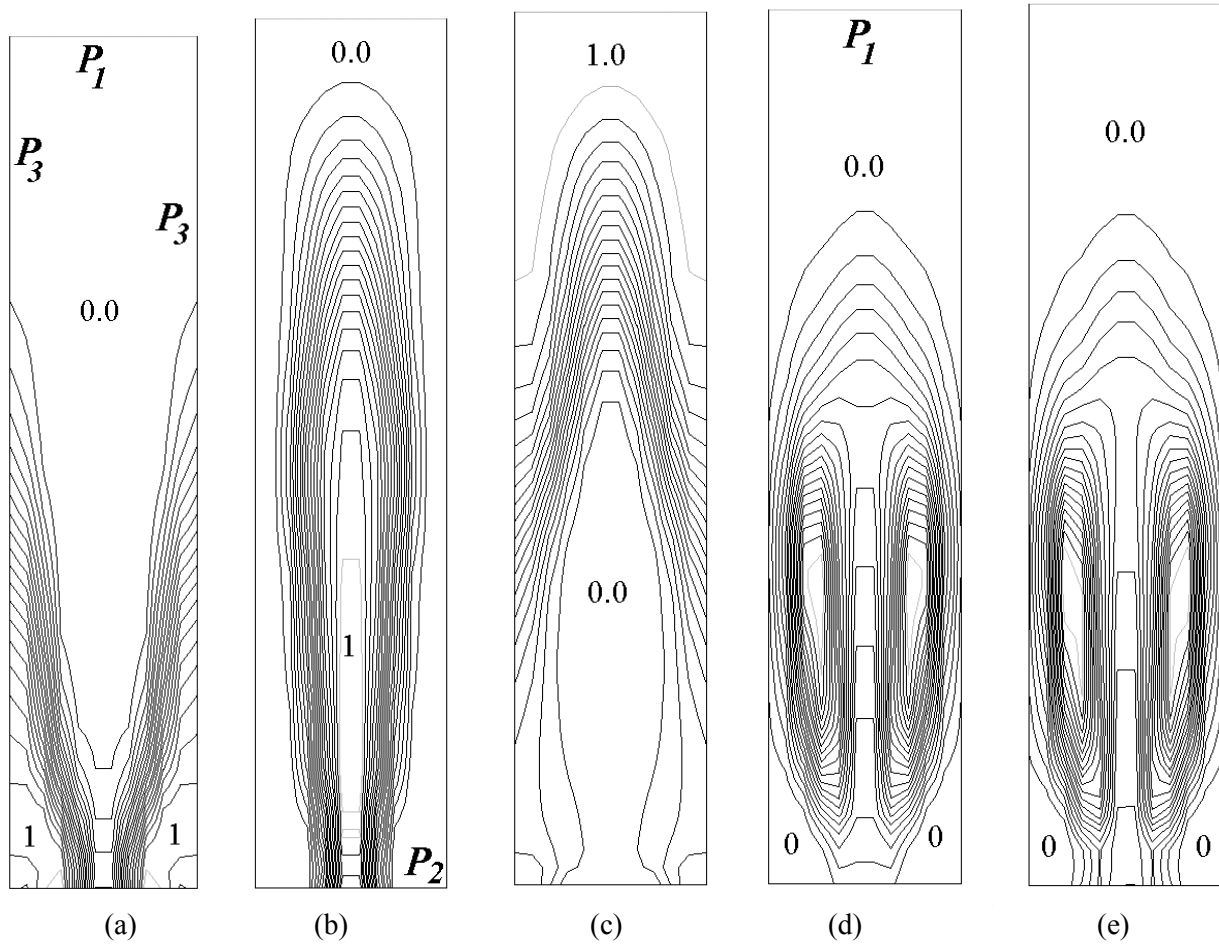


Fig. 9. Mass concentration isolines of methane (a), oxygen (b), nitrogen (c), CO_2 (d) and H_2O (e) at instant $t = 2,0 \cdot 10^{-4}$ s.

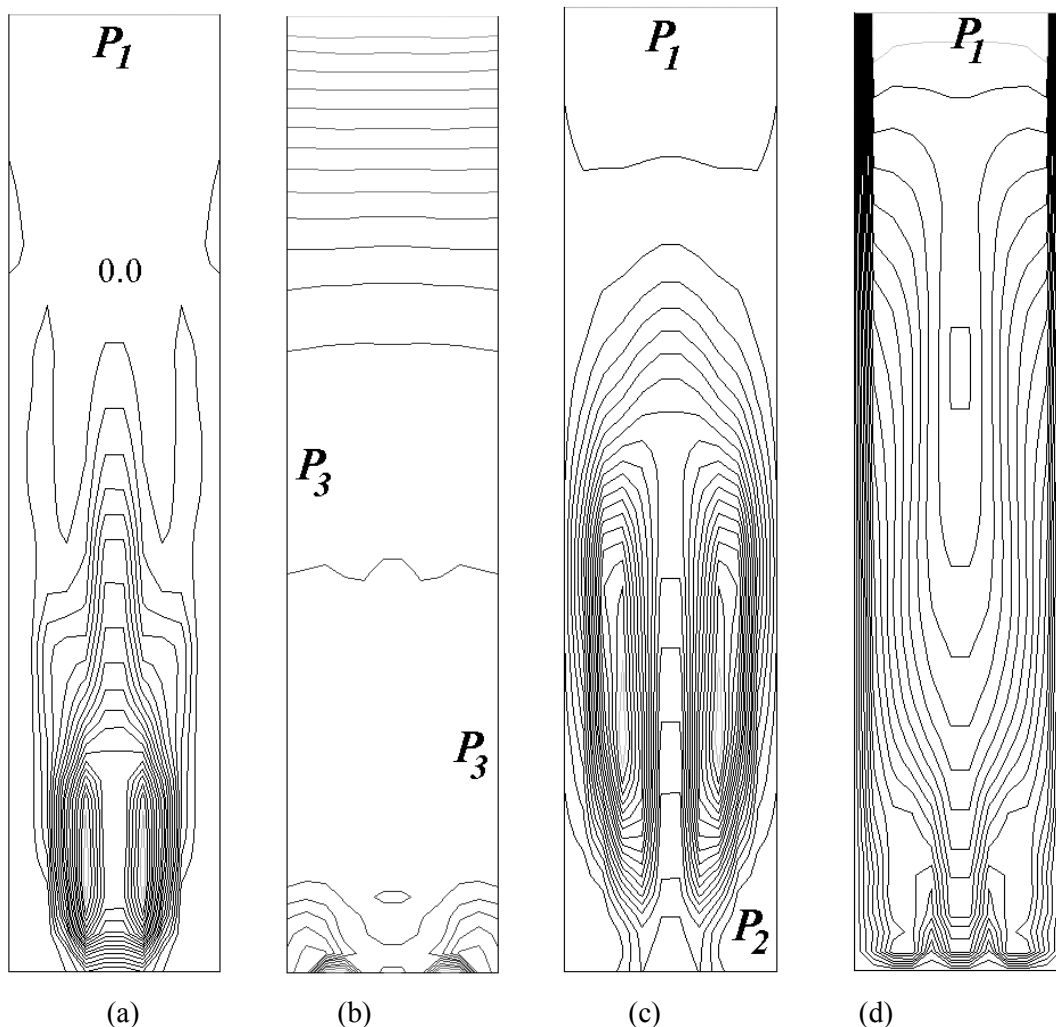


Fig. 10. Isolines of rate of chemical reaction (a, $\text{kg}\cdot\text{moll}/(\text{m}^3 \text{ s})$), pressure (b), temperature (c) and velocity (d) at instant $t = 2,0 \cdot 10^{-4}\text{s}$.

Contribution of Individual Authors to the Creation of a Scientific Article (Ghostwriting Policy)

The author contributed in the present research, at all stages from the formulation of the problem to the final findings and solution.

Sources of Funding for Research Presented in a Scientific Article or Scientific Article Itself

No funding was received for conducting this study.

Conflict of Interest

The author has no conflict of interest to declare that is relevant to the content of this article.

Creative Commons Attribution License 4.0 (Attribution 4.0 International, CC BY 4.0)

This article is published under the terms of the Creative Commons Attribution License 4.0

https://creativecommons.org/licenses/by/4.0/deed.en_US